AIMS Geosciences, 3 (4): 498-513
DOI: 10.3934/geosci.2017.4.498
Received date 30 June 2017
Accepted date 22 September 2017
Published date 29 September 2017

http://www.aimspress.com/journal/geosciences

Research article

Inactivation of Bacterial Spores and Vegetative Bacterial Cells by Interaction with ZnO-Fe_2O_3 Nanoparticles and UV Radiation

José Luis Sánchez-Salas [1,*], Alejandra Aguilar Ubeda [1], Beatriz Flores Gómez [1], Oscar Daniel Máynez Navarro [1], Miguel Ángel Méndez Rojas [1], Silvia Reyna Tellez [1], and Erick R. Bandala [2]

[1] Department of Chemical and Biological Sciences. Sciences School. Universidad de las Américas Puebla. Ex-Hacienda de Santa Catarina Mártir. C.P. 72810. Cholula, Puebla, México

[2] Division of Hydrologic Sciences, Desert Research Institute. Las Vegas, Nevada, USA

*** Correspondence:** Email: jluis.sanchez@udlap.mx.

Abstract: ZnO-Fe_2O_3 nanoparticles (ZnO-Fe NPs) were synthesized and characterized by scanning electron microscopy (SEM), energy dispersive X-ray spectroscopy (EDS) and dynamic light scattering (DLS). The generation of chemical reactive hydroxyl radicals ($^{\bullet}OH$) was measured spectrophotometrically (UV-Vis) by monitoring of *p*-nitrosodimethylaniline (*p*NDA) bleaching. Inactivation of *E. coli* and *B. subtilis* spores in the presence of different concentrations of ZnO-Fe NPs, under UV_{365nm} or visible radiation, was evaluated. We observed the best results under visible light, of which inactivation of *E. coli* of about 90% was accomplished in 30 minutes, while *B. subtilis* inactivation close to 90% was achieved in 120 minutes. These results indicate that the prepared photocatalytic systems are promising for improving water quality by reducing the viability of water-borne microorganisms, including bacterial spores.

Keywords: Drinking water; nanoparticles; photocatalysis; hydroxyl radicals; zinc oxide; iron oxide; Bacterial inactivation; Bacterial spore inactivation

1. Introduction

Clean drinking water is considered a human right by the UN through its Resolution 64/292 [1], however, currently there are high levels of inequality relative to clean water distribution, mainly in developing countries. The World Health Organization (WHO) reported in 2006 that around 40% of total population has no access to safe and clean drinking water [2]. Social programs and economic resources intended to improve the water quality and/or its distribution have not been enough to reach the goals established by global organizations, including those recommended by WHO [3]. In the other hand, it is well-known that unsafe water can transport different kinds of water-borne pathogens like bacteria (*Salmonella spp., Shigella spp., Campylobacter spp., Escherichia coli, Bacillus cereus*), virus (*virus norwalk, rotavirus y adenovirus, hepatitis A virus*), and protozoa (*Cryptosporidium parvum, Giardia lambia, Entamobeahistolyitica*) [4]. A recent study of Bain *et al.* [5] estimated that approximately 1.8 billion people globally use a source of drinking water containing fecal contamination. It has been estimated that nearly 10% of water sources may be of "high" risk, containing at least 100 *E. coli* or thermotolerant coliform per 100 mL. In that study, the authors indicated that fecal contamination is most prevalent in Africa and South-East Asia, affecting all water source types including water supplied in pipes.

In 2014, Prüss-Ustün*et al.* [6] found that in the year 2012, an estimated of 502 000 diarrhea deaths were caused by inadequate drinking water and more than 280 000 deaths by inadequate sanitation. Around 361 000 deaths of children under 5 years old could be prevented, representing 5.5% of deaths in that age group. Their estimations confirm the importance of improving water quality and sanitation in low–and middle-income settings for the prevention of diarrheal disease burden. It also underscores the need for better data on exposure and risk reductions that can be achieved with provision of reliable piped water, community sewage with wastewater treatment and hand hygiene. In addition, according to the study of Wolf *et al.* [7], inadequate water and sanitation are associated with increased risks of diarrheal disease and with notable differences in illness reduction according to the type of improved water and sanitation implemented. In the other hand, all systems to provide safe water must consider first to produce clean water.

There are different procedures to produce good quality drinking water, but most of them are expensive or inefficient. Chlorination is a good example, which, although it is one of the most used methods for cleaning water, it cannot be applied at any situation. Some bacteria like *Listeria* and *Bacillus subtilis* are resistant to up 150 ppm of chlorine, and in presence of organic matter, others like *Yersinia* and *E. coli* turn resistant to the same concentration of chlorine [8]. The need to find alternative procedures to obtain clean water is in the rise, and advanced oxidation processes (AOPs) are among the newest available. AOPs for pathogen inactivation has emerged recently as a cost-effective alternative for safe drinking water production. Different AOPs methodologies using ozone [9,10], UV radiation [11], and photo-Fenton reaction [12,13] have demonstrated the viability of these technologies for the inactivation of pathogens in water. However, most of the photocatalytic

materials need to use UV light to produce oxidant species like hydroxyl radical in order to inactivate microorganisms. Then, one of the main challenges is to modify these materials to extend its range into the visible light spectrum in order to improve these processes. Taking advantage of new nanomaterials and their different and unique properties, nanostructured photocatalysts can be considered a useful alternative to clean water and they could be adaptable to any low- or middle- community by using solar energy.

Here, we developed and characterized ZnO-Fe_2O_3 nanoparticles (ZnO-Fe NPs); the photo-bleaching of *p*-nitrosodimethylaniline (*p*NDA) was spectrophotometrically followed to determine the amount of hydroxyl radicals produced, as well as their ability to inactivate *E. coli* and *B. subtilis* spores using UV_{365nm} or white-light irradiation.

2. Materials and Methods

2.1. Reagents

All the reagents (zinc acetate dihydrate, iron(III) acetylacetonate, NaCl, NH_4OH, isopropanol) were reagent grade obtained from Sigma-Aldrich Co., and used as received without any further purification. Triple distilled water (DI) was used in all preparations.

2.1.1. Sol-Gel ZnO-Fe NPs synthesis

The synthesis was performed as described previously by Maya-Treviño, *et al.* [14] and Hasnidawani, *et al.* [15] with some modifications. A mixture of zinc acetate dihydrate (0.0.6 mol) in 210 mL of distilled water and 0.55 percent of iron (II) acetylacetonate, previously dissolved in 40 mL of isopropyl alcohol, was prepared. Then, a concentrated NH_4OH solution was added to the mixture under continuous stirring, and the pH was adjusted to 8 (pH meter, Conductronic, PC18). The reaction mixture was maintained at room temperature until gelification. The gel was aged for 3 days and later dried in an oven (Riossa, E-33) at 75 ^oC (fresh sample). Finally, the product was calcined using an electrical furnace (Thermolyne, F48025) at 450 ^oC for 4h. With this procedure, approximately 4.0 g of material were obtained. Before using these nanoparticles, they were sonicated by 15 minutes using a continuum mode with an amplitude of 100 units (Sonics, VC 130PB).

2.1.2. Characterization of ZnO-Fe NPs

Morphological analyses were performed using a FEI Scios DualBeam scanning electron microscope (SEM) at 20 kV, coupled with energy dispersive spectroscopy (EDS). Samples were deposited on top of a graphite conductive tape on an aluminum pin and dried before analysis. The

aggregate particle size distribution was determined *via* dynamic light scattering (DLS) using a Nanotrac Wave (Microtrac) instrument, working at 28 °C with DI water as dispersing media, using a 3 mW red laser (780 nm). Finely powdered samples were dispersed using an ultrasonic bath (5 min) in DI water and then analyzed during 60 seconds to collect data for size distribution analyses.

2.2. Hydroxyl radical generation assessments

To get evidence of $^{\bullet}OH$ participation in spore inactivation, *p*NDA was used as an $^{\bullet}OH$ scavenger based on results from previous works [16–18]. It is widely known that *p*NDA is used as a scavenging agent to selectively trap hydroxyl radicals as it does not react with the other ROS species (singlet oxygen, $^1O_2$; superoxide anions, O_2^-; or other peroxy compounds). Because *p*NDA is sensitive to pH changes, the 10 µM *p*NDA test solution was prepared and initially adjusted to pH 6.0 ± 0.1 using NaOH or HCl as needed [19]. No buffer solution was used because it could compete with the *p*NDA scavenger for generated $^{\bullet}OH$ radicals. The end value of pH for the reaction was verified using the pH of the discharged *p*NDA bleaching mixture. Bleaching of *p*NDA was measured using a UV-visible spectrophotometer (Hatch DR/4000U) at 440 nm. N,N-dimethyl-4-nitrosoaniline bleaching has been demonstrated to be useful for measuring the photocatalytic performance of TiO_2 [20,21]. This method also has some advantages, such as: (1) selectivity of the reaction of *p*NDA with $^{\bullet}OH$ [22]; (2) high reaction rate between *p*NDA and $^{\bullet}OH$ on the order of 10^{10} M^{-1} s^{-1} [18,23]; (3) easy to observe bleaching at 440 nm following Beer's Law; and (4) 1:1 stoichiometry, which means that one $^{\bullet}OH$ can bleach one *p*NDA molecule [16–18,24], as described in Equations (1) and (2):

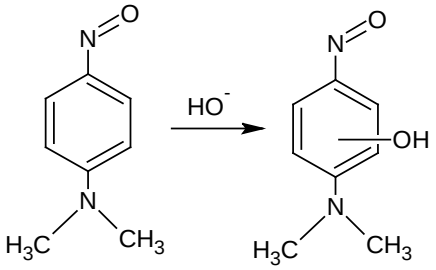

(1)

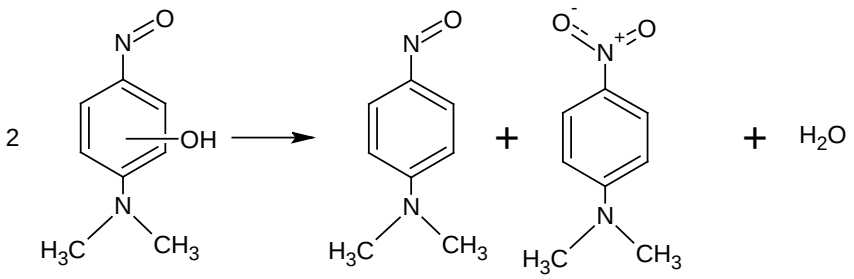

(2)

In summary, 0.1 g of ZnO-Fe NPs and 1.0 mL of 0.1 mM *p*NDA, were dispersed in 100 mL of distillated water. The mix was transferred into a 250 mL beaker containing a magnetic bar and kept inside of a dark box illuminated by two UV_{365nm} lamps of 15 W (Technolite, F15T8BLB), under continuous magnetic stirring (Cole Parmer, 03402-10) at moderate speed. 4 mL aliquots were taken at 30, 60, 90, 120 and 150 min and stored into 15 mL conic plastic tubes, wrapped in aluminum foil and stored in a dark closed box to reduce the effect of residual light. All collected samples were centrifuged at 5600 rpm and 3 mL were taken to measure the absorbance at 440 nm as mentioned before. To determine the hydroxyl radical generation efficiency by ZnO-Fe NPs, the statistic software R was used to fit the data into a linear equation, as indicated by equation (3):

$$\%BE = \frac{A_o - A_t}{A_o} \qquad (3)$$

Where *BE* is the bleaching efficiency, A_o is the initial absorbance and A_t being the final absorbance for each time.

2.3. Bacterial and bacterial spore

In order to evaluate the properties of ZnO-Fe NPs to inactivate bacterial cells or spores, a fresh culture of *Escherichia coli* ATCC 25922 (vegetative cell standard) and spores of *Bacillus subtilis* (strain 169) were used. *E. coli* and *B. subtilis* were obtained from the strain collection of the Laboratory of Microbiology at Universidad de las Americas Puebla, where they are stored a -80°C in nutrient broth plus 20% of glycerol. One frozen sample of each strain was streak on a Petri dish containing nutritive agar (Bioxon) and incubated overnight at 37 °C. *E. coli* then was subcultured on MacConkey agar to confirm its morphology and lactose positive reaction. Later, it was cultured on 10 ml of liquid nutrient broth overnight to have the culture on logarithmic phase to use in each assay. Before its use, the culture was centrifuged at 5000 rpm for 10 min and the pellet rinsed with saline isotonic sterile solution (NaCl 0.85%) and adjusted to the tube No 1 of the MacFarland Nephelometer corresponding to ~ $3 * 10^8$ cells mL^{-1} [25]. To isolate spores of *B. subtilis*, they were obtained using the method previously described by Sanchez-Salas, *et al.* [26]. Few colonies were streak on 250 mL of 2xSG medium in a 1L Erlenmeyer flasks (4 flasks) and incubated for 3 to 5 days at 37 °C on a water bath shaker until 80–90% of spores are released from mother cells. The spores were harvested by centrifugation at 5600 rpm for 20 min at 4 °C and all pellets were pooled in two 50 mL conical plastic tubes. The spores were suspended in 10 times its volume with cold water (4 °C). The spores were rinsed daily for 10 to 15 days until less of 2% are cells or cell detritus. The concentration of spores was measured by using the absorbance at 600nm as reported previously [17]. Spores were stored at 4 °C in distillated water.

2.4. Vegetative and bacterial spore inactivation

For UV irradiation, a non-microbicide UV lamp (UV_{365nm}) of 100 Watts was located at 20 cm from the Petri dish bottom (UV_{365nm} lamp of 15 Watts at a distance of 10 cm). For white light, two fluorescent light lamps of 15 Watts (Technolite, F15T8D) were positioned at 10 cm of distance. Before the cell and spore inactivation, a Petri dish containing 20 mL of distillated water, ZnO-Fe NPs (0.5, 0.05 and 0.005 mg mL^{-1}), and a magnetic stirring bar was sterilized using a UV lamp (260 nm) into a sterile Gard III cabinet (Advance SG-303) for 30 min. After that, the Petri dish was set on a magnetic stirrer plate (Cole Parmer, 03402-10) at slow speed. For *E. coli*, 100 μL from the adjusted inoculum (~ $3 * 10^8$ cells mL^{-1}) was added to the Petri dish containing ZnO-Fe NPs and for *B. subtilis* 100 μL from a spore suspension with an initial optical density of 1.0 (600 nm) was used. After the addition of cells or spores into the Petri dish, a 100 μL aliquot was taken and added into 900 μL of saline isotonic sterile solution (SISS) and label as t_0. Then the lamp was turned on and consecutive different aliquots were taken at 1, 3, 5, 10, 15, 30, 60, 90 and 120 min for each assay. Each sample was diluted several times (1:10) until $1 * 10^7$ using SISS. Afterwards, from each dilution, 10 μL were spotted by duplicated on nutrient agar for *E. coli* and LB agar for *B. subtilis*. All plates were incubated at 35 °C for up to 24 h, although colony formation was invariably complete in ~ 16 h, and colonies were counted. Considering that the numbers of colonies correspond to number of cells because each cell after incubation develops a colony, all plots are related to number of cells. All the experiments were conducted in dark space. As a control was used the same dark conditions but without any light source. All experiments were made by triplicated and the results are the average of all three. Because the numbers of cells in the beginning of each experiment are different, all calculation were normalized using the equation (4):

$$N_t/N_0 \qquad (4)$$

Where N_0 is the initial number of cells at the beginning of the assay and N_t is the final number of cells at the time t analyzed. Afterwards, the natural logarithm of all curves where calculated to obtain the slope of each time and calculate the inactivation rate constant k_i. The inactivation efficiency was also calculated using equation (5):

$$IE = \frac{N_o - N_t}{N_o} * 100 \qquad (5)$$

Where IE is the inactivation efficiency, N_0 is the number of cells at time zero and N_t the number of cells at the end of each time t. ANOVA analysis of the data was done and the R software to find any significant difference. All controls (no radiation, UV_{365nm} radiation, white light and ZnO-Fe NPs) were used alone to compare its effect with the combination conditions. It is important to mention that ZnO alone, has shown antibacterial activity and can be enhanced by UV_{365nm} or white light radiation [27]. All experiments were done by triplicate and only the average are shown.

3. Results and discussion

3.1. Characterization of ZnO-Fe NPs

The morphology and dimensions of the nanostructured photocatalysts were studied by SEM; a selected image of the as-prepared NPs is shown on Figure1 NPs are less than 100 nm, forming agglomerates through interaction of several smaller particles. The average size, after measuring nearly 100 independent particles, was of 102.7 ± 10.5. The shape of these NPs is irregular and no pores are visible. The chemical composition of the nanoparticles was analyzed using EDS, showing the presence of both metals (Zn and Fe) in the sample, as well for O, as expected for the ZnO-Fe_2O_3 nanoparticles (ZnO-Fe NPs).

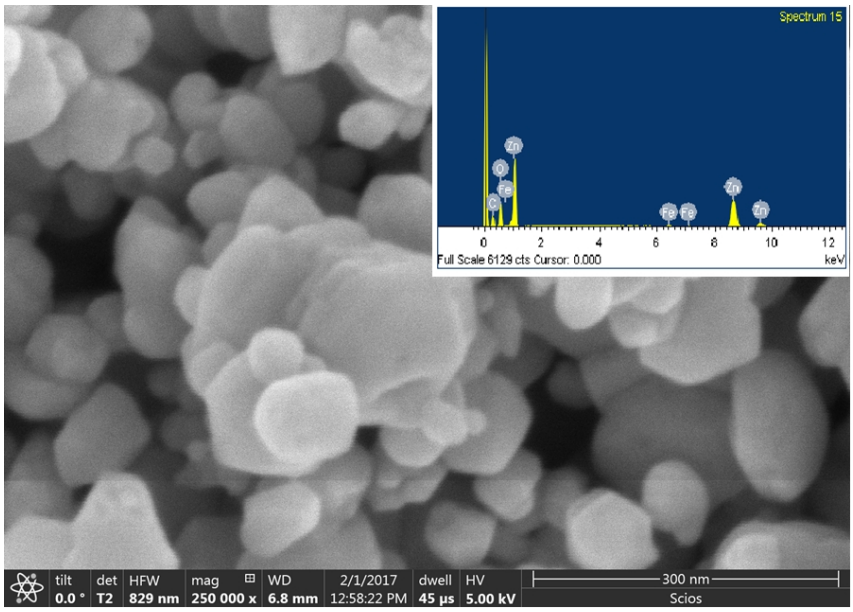

Figure 1. SEM micrograph of ZnO-Fe NPs. Inset shows the EDS spectrum.

By using DLS, the relative particle size distribution in solution of the NPs was determined. The particle size distribution in DI water of the dried (at 75 °C) nanoparticles was in the range between 60 and 480 nm, having an average size less than 100 nm. After calcination (at 450 °C) particles dispersed in DI water showed a size distribution from 85 to 400 nm, with an average size that was also less than 100 nm (Figure 2). No significant changes in size distribution were observed for the obtained NPs, before and after calcination, although it was clear that the NPs trend to agglomerate in solution as a result of the lack of a surfactant to stabilize them. Agglomeration may cause a diminution on the active superficial area, affecting the photocatalytic performance.

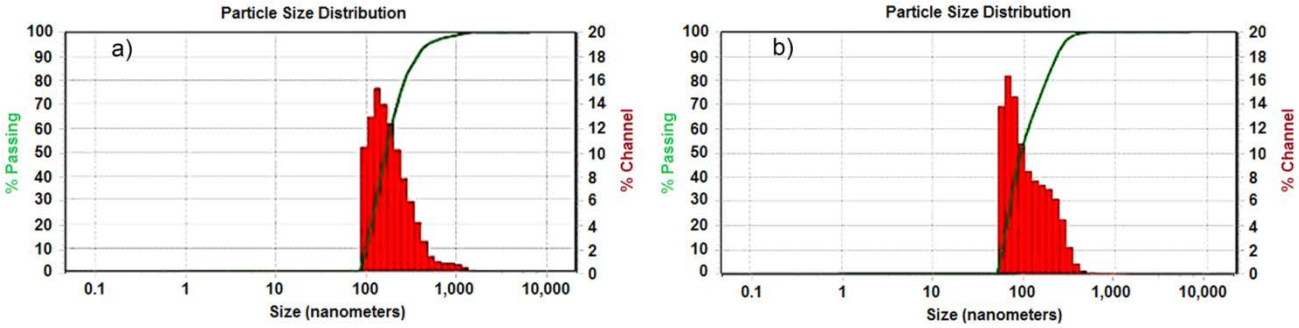

Figure 2. Particle size distribution of (a) ZnO-Fe NPs without calcination and (b) ZnO-Fe NPs after calcination at 450^{0}C, as determined by DLS.

3.2. pNDA photo-bleaching by ZnO-Fe NPs

Calcinated ZnO-Fe NPs were used as photocatalysts to bleach *p*NDA in water under UV_{365nm} irradiation. As seen in Figure 3, nearly 35% of *p*NDA was bleached after 150 min. The estimated hydroxyl radical production was 0.0354 µm min^{-1}. These results confirm the photoactivity of these NPs under UV_{365nm} light.

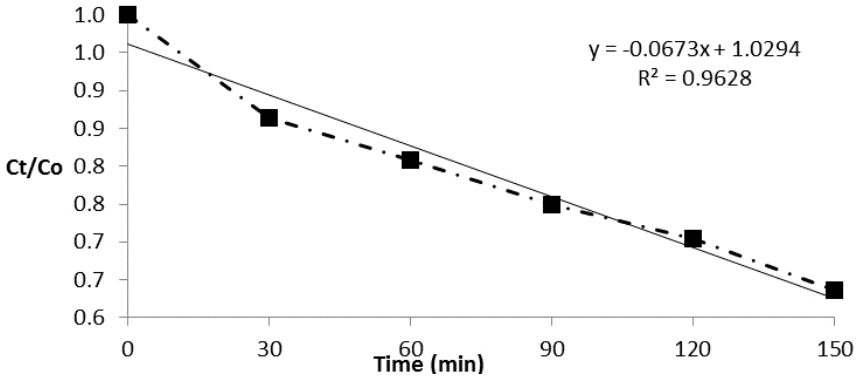

Figure 3. Bleaching of pNDA (1µM) using ZnO-Fe using UV_{365nm} light.

3.3. Vegetative cells inactivation using different irradiation sources

The first assay was made by only using an irradiation source. *E. coli* under UV_{365nm} light using a 15 W lamp located at a distance of 10 cm or at 20 cm of a 100 W lamp (576 µW cm^{-2}) showed a total cells reduction of ~36% after 120 min. These results are similar to previous report of the low antibacterial effect of UV radiation with a wavelength close of the visible wave length [27]. In contrast and as expected, under white light irradiation (15 W, 10 cm) shows no inactivation of *E. coli*. Not using an irradiation source has no significant change on *E. coli* population, as shown on Figure 4.

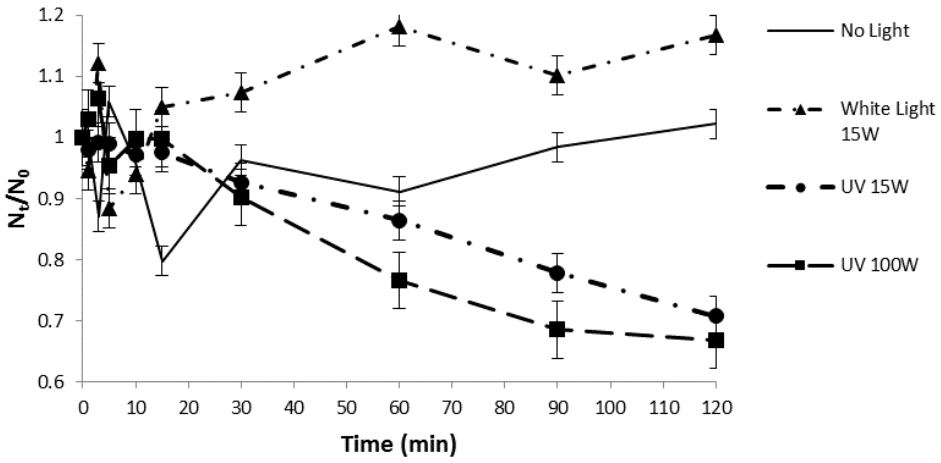

Figure 4. *E. coli* inactivation using different types of radiation.

Next, testing the effect of ZnO-Fe NPs of on the number of cells of *E. coli* was evaluated. As shown on Figure 5a, the number of *E.coli* cells is affected negatively by the presence of ZnO-Fe NPs without light irradiation. This can be explained by liberation of Zn(II) ions in the medium, which have been reported to possess antimicrobial activity [28]. After 15 minutes, a significant reduction of the number of cells was observed, being more notorious the effect for ZnO-Fe NPs concentrations of 50 and 500 μg mL^{-1}. Up to 90% of inactivation was achieved this way, with no further improvement after 15 minutes. Approximately 90% of inactivation was achieved after 30 min with a concentration of 5 μg mL^{-1} (Figure 5b). This can be explained by the generation of ROS by the ZnO-Fe NPs which in turn can oxidize *E. coli* cell membrane, which is a process dependent of the NPs concentration as reported by Jones *et al* [27] or Achouri *et al.* [29].

The first set of tests used a highly energetic light source (UV_{365nm} at 100 W), 20 cm apart, and as expected, *E. coli* had a better inactivation rate after the first 60 min as shown previously on Figure 4. By combining an irradiation source with exposition to ZnO-Fe NPs, almost 100% *E. coli* inactivation was achieved at any concentration used this way. This indicates that even at the lowest concentration of ZnO-Fe NPs (5 μg mL^{-1}) *E. coli* inactivation is almost complete when using a 100 W UV_{365nm} light after 60 min as shown on Figure 5b. In contrast, when using a 15 W UV_{365nm} lamp positioned 10 cm apart of the sample, 90% of the cells were inactivated at the highest concentration (500 μg mL^{-1}) of ZnO-Fe NPs after 30 min. The same result was achieved after 60 min when using 50 μg mL^{-1} of NPs. Using a 15 W UV_{365nm} lamp, the lowest concentration (5 μg mL^{-1}) could inactivate 90% of the cells after 90 min, as shown in Figure 5c. That suggest that *E. coli* can be inactivated using UV_{365nm} light source of different intensities. The previous results were promising, but as ZnO-Fe NPs have a different band-gap than ZnO NPs, the next set of tests were focused on achieving inactivation using common white light sources. Surprisingly, 90% of inactivation was obtained with 500 μg mL^{-1} of ZnO-Fe NPs, after only 10 min. Using the lowest concentration (5 μg mL^{-1}), *E. coli* was fully inactivated after 90 min with white light irradiation. These results are shown on Figure 5d.

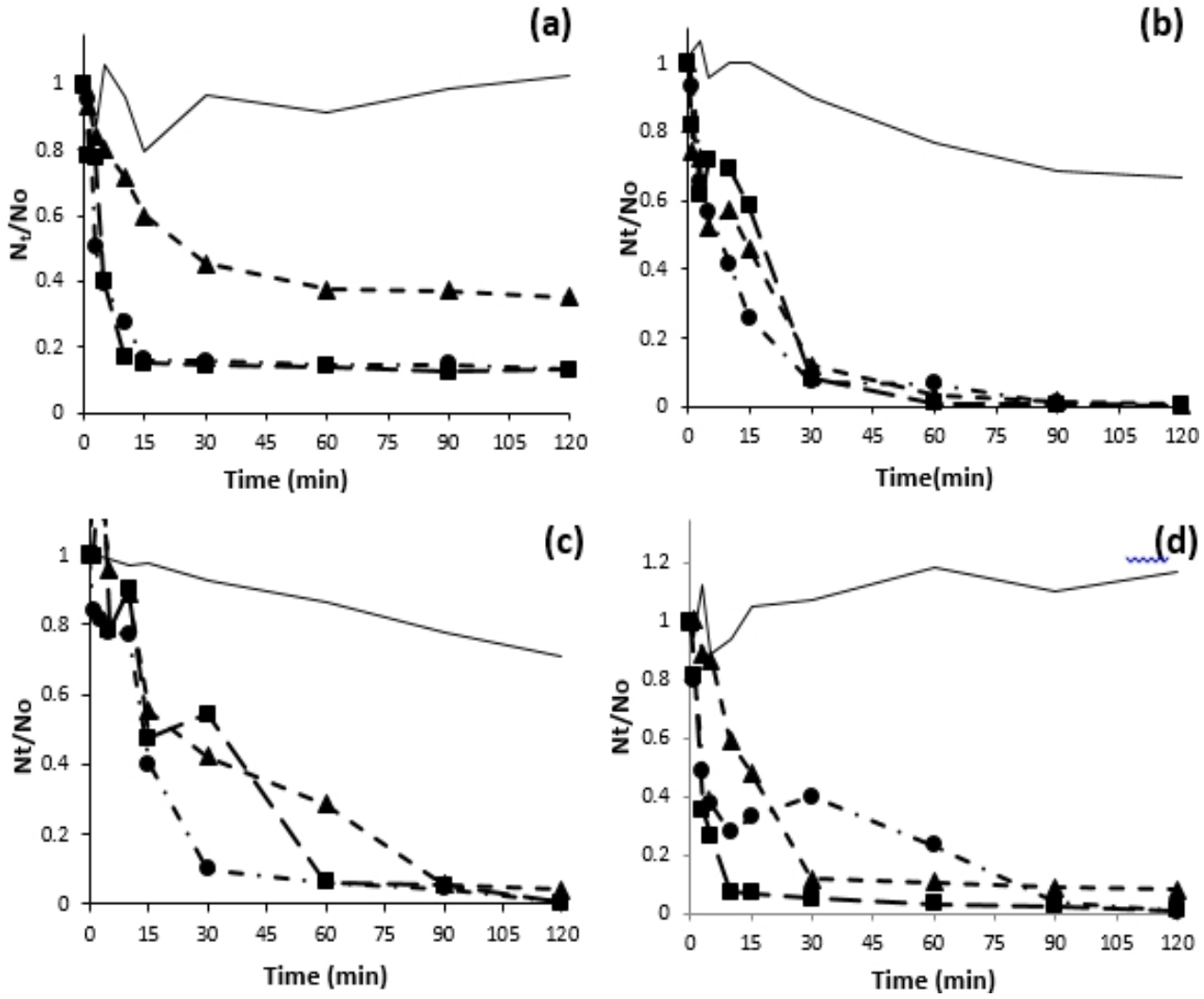

Figure 5. ***E. coli*** **inactivation using different light sources (a) no irradiation; (b) UV_{365nm} 100W; (c) UV_{365nm} 15W; (d) white light 15W, and with different ZnO-Fe concentrations (—: no ZnO-Fe; ▲: 5 g mL^{-1} ZnO-Fe; ●: 50 g mL^{-1} ZnO-Fe; ■: 500 g mL^{-1} ZnO-Fe).**

Comparison between the different light sources and using the lowest concentration of ZnO-Fe NPs is shown on Figure 6. It can be seen that using no light has no significant effect on *E. coli* inactivation, being only 65% after 120 min. It was observed that bacterial inactivation was larger when white light was used that when UV_{365nm} 15W, which can be attributed to modifications of the electronic structure (band-gap) of the ZnO-Fe_2O_3 nanoparticles (ZnO-Fe NPs). All light sources showed their best performance after 90 min, with inactivation of 90% or more for all cases.

Assays for evaluation of *B. subtilis* inactivation where performed under the same conditions as previously described for *E. coli*. In the first test we used different light sources, including no light source, and without NPs exposure. Figure 7 shows these results, indicating that there were no significant inactivation effects on *B. subtilis* spores.

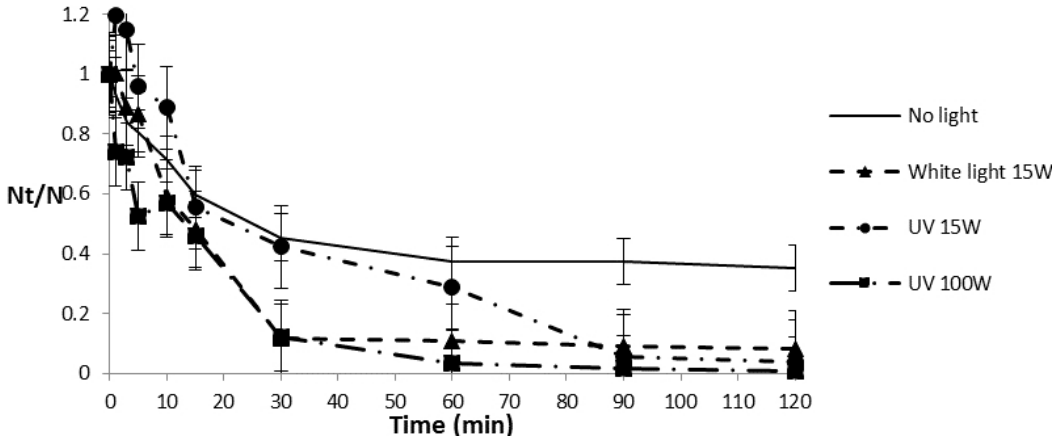

Figure 6. Comparison of *E. coli* inactivation by using 5 g $mL^{-1}$of ZnO-Fe NPs and different types of radiation.

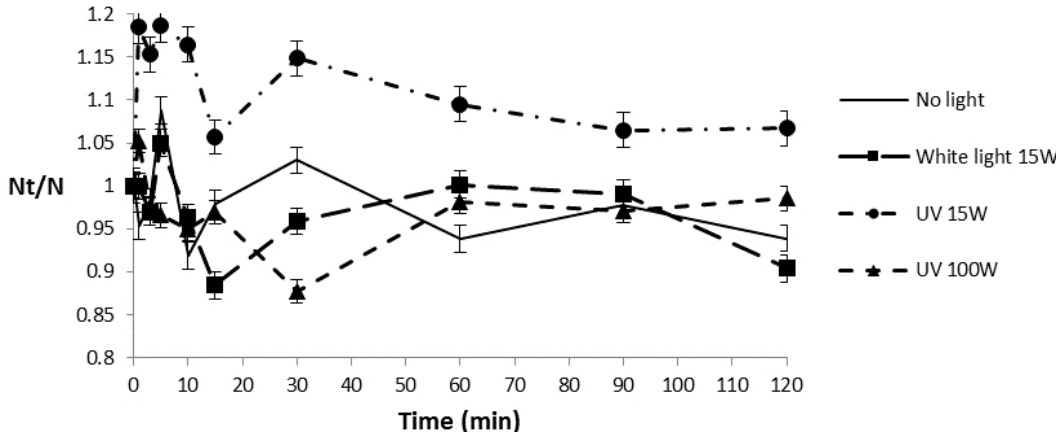

Figure 7. *B. subtilis* inactivation using different types of radiation.

Using ZnO-Fe NPs resulted in less toxicity on *B. subtilis* spores than with *E. coli*. A concentration of 500 μg mL^{-1} of NPs inactivated 50% of the spores after 60 min. Lower concentrations (50 or 5 μg mL^{-1}) reduced only 20% of the spores after 120 min, as shown on Figure 8a. When a high-energy irradiation source was added (Figure 8b), significant effects were observed. Using a 100 W UV_{365nm} lamp combined with a concentration of 500 μg mL^{-1} of NPs achieved 70% of *B. subtilis*spores inactivation after 120 min of irradiation. This effect is caused mainly by the toxicity of ZnO-Fe NPs rather than the UV_{365nm} irradiation, as ZnO-Fe NPs alone showed to produce almost the same effect than the ZnO-Fe NPs coupled with UV_{365nm}. We have seen that ZnO NPs can reduce the germination rate of *B. subtilis* spores (data not published). When 0.005 mg mL^{-1} were used, inactivation was observed after the first 30 min, but an increase of spore count was observed after 60 min. When a lower potency light source, a 15 W UV_{365nm} lamp, was used (Figure 8c), inactivation results similar to

those previously seen for *E. coli* were obtained. With 500 and 50 μg mL^{-1} NPs concentrations, spore inactivation of 65% were achieved, after 60 and 90 min, respectively. It should be noted that 50% of inactivation was reached after only 30 min when using 500 μg mL^{-1} of ZnO-Fe NPs. The lowest concentration (5 μg mL^{-1}) could only achieve 20% of the inactivation after 120 min. When a common white light source was used, inactivation of *B. subtilis* spores was less than when using UV_{365nm} light, as expected. The lowest concentration of NPs (5 μg mL^{-1}) barely inactivated 10% of the spores after 120 min, while using a concentration of 50 μg mL^{-1} of NPs achieved 30% after the same time. However, when using the highest concentration of NPs (500 μg mL^{-1}), 50% of the spores were inactivated after 45 min, and 90% inactivation was reached after 120 min. These results are shown on Figure 8d.

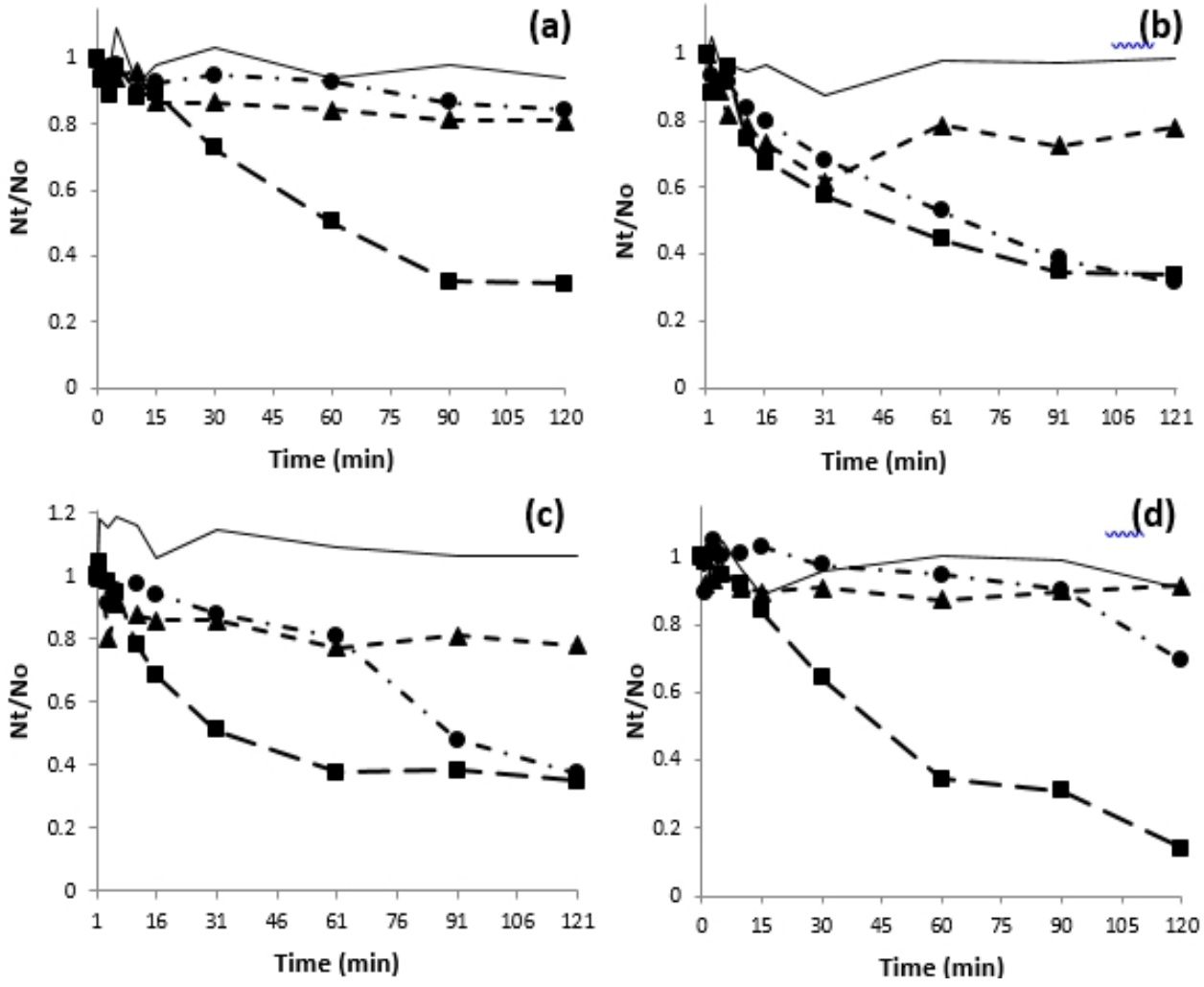

Figure 8. *B. subtilis* inactivation using different light sources (a) no irradiation; (b) UV_{365nm} 100W; (c) UV_{365nm} 15W; (d) white light 15W, and with different ZnO-Fe concentrations (—: no ZnO-Fe; ▲: 5 g mL^{-1} ZnO-Fe; ●: 50 g mL^{-1} ZnO-Fe; ■: 500 g mL^{-1} ZnO-Fe).

Comparison between the different light sources and using the highest concentration of ZnO-Fe NPs is shown on Figure 9. This concentration was used to compare, as it could achieve 65–70% spore inactivation for almost all tests after 120 min. White light irradiation had the best performance, having almost full inactivation in that period of time. Toxicity of ZnO-Fe is similar to ZnO NPs alone, as published by Jones *et al* [27]. As stated by Jones *et al*, such antibacterial effect is due to the ROS produced by this material. However, more than one mechanism that explain the antibacterial activity can exist. In the other hand, it is well known that bacterial spores are much more resistant than vegetative cells mainly by its content of SASP, protein which protect the DNA to UV_{260nm} light [30], which is more effective as an antimicrobial agent than UV_{365nm} [31].

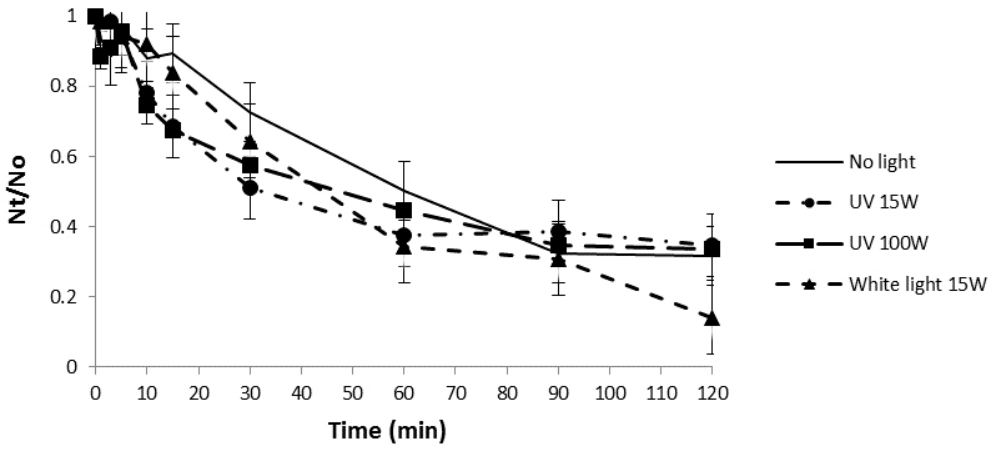

Figure 9. Comparison of *B. subtilis* inactivation by using 500 g mL^{-1} of ZnO-Fe NPs and different types of radiation.

4. Conclusion

In this work, the preparation of ZnO-Fe_2O_3nanoparticles (ZnO-Fe NPs), was completed successfully. The physical and chemical analysis are in agreement with the expected product. Particle size is in the range between 85 to 400 nm, with a trend to agglomerate in solution. ZnO-Fe NPs are photocatalytically active under UV_{365nm} and white light irradiation. As expected, these NPs had good performance for *p*NDA photo-bleaching, indicating that hydroxyl radical are produced during the photochemical activation, in agreement with the original hypothesis that ROS are responsible for bacterial (vegetative or spore structure) inactivation. The inactivation of *E. coli* cells and *B. subtilis* spores is dependent of the irradiation source, which creates free radicals that synergizes with the toxicity of the ZnO-Fe NPs themselves. All previous results are of great interest because is known that ZnO alone can be toxic to different types of cells for its ability to produce hydroxyl radicals, so, doping the material has a favorable effect on increasing the wavelength range needed to achieve photoactivation. Further research on inactivation mechanistic pathways and the cytotoxic effect of

the nanoparticles are underway, in order to optimize these systems, and to have a better understanding of the potential negative effects they may have on human consumption.

Acknowledgement

The authors are thankful to Dr. Netzahualcoyotl Carlos at the Electron Microscopy Laboratory at National Institute of Astrophysics, Optics and Electronics (INAOE) for help with SEM/EDS analysis.

Conflict of interest

All authors declare no conflicts of interests in this paper.

References

1. United Nations General Assembly, Resolution 64/292. The human right to water and sanitation 2010. Available from: http://www.un.org/es/comun/docs/?symbol=A/RES/64/292&lang=E.
2. World Health Organization, Meeting the MDG drinking water and sanitation. The urban and rural challenge of the decade, UNICEF, 2006. Available from: http://apps.who.int/iris/bitstream/10665/43488/1/9241563257_eng.pdf?ua=1.
3. World Health Organization, Global status report on noncommunicable diseases, WHO, 2010.
4. J Doménech (2003) *Cryptosporidium* y *Giardia*, problemas emergentes en el agua del consumo humano. *Offarm: Farm Soc* 22: 112-116.
5. R Bain, R Cronk, R Hossain, et al. (2014) Global assessment of exposure to faecal contamination through drinking water based on a systematic review. *Trop Med Int Health* 19: 917-927.
6. A Pruss-Ustun, J Bartram, T Clasen, et al. (2014) Burden of disease from inadequate water, sanitation and hygiene in low- and middle- income settings: a retrospective analysis of data from 145 countries. *Trop Med Int Health* 19: 894-905.
7. Wolf J, Pruss-Ustun A, Cumming O, et al. (2014) Assesing the impact of drinking water and sanitation on diarrhoeal disease in low- and middle-income settings: systematic review and meta-regression. *Trop Med Int Health* 19: 928-942.
8. Virto R, Mañas P, Álvarez I, et al. (2005) Membrane damage and microbial inactivation by chlorine in the absence and presence of a chlorine-demanding substrate. *Appl Environ Microbiol* 71: 5022-5028.
9. MT Orta, J Martínez, I Monje, et al. (2004) Destruction of helminth (*Ascaris summ*) eggs by ozone. *Sci Eng* 26: 359-366.
10. MT Orta, MN Rojas, M Vaca. Destruction of helminth (*Ascaris suum*) eegs by ozone: second stage. *Wat Supply* 2: 227-233.

11. Z Alouini, M Jemli (2004) Destruction of helminth eggs by photosensitized porphyrin. *J Environ Monit* 3: 548-551.
12. ER Bandala, MA Peláez, DD Dionysiou, et al. (2007) Degradation of 2,4-dichlorophenoxyacetic acid (2,4-D) using cobaltperoximonosulfate in Fenton-like process. *J Photochem Photobiol A* 186: 357-363.
13. RM Ramírez, M Galvan, I Retama, et al. (2006) Viability reduction of parasites (*Ascaris spp.*) in water with photo-Fenton reaction via response surface methodology. *Wat Pract Technol* 1: 120-125.
14. ML Maya-Treviño, JL Guzmán-Mar, L Hinojosa-Reyes, et al. (2014) Activity of the ZnO-Fe_2O_3 catalyst on the degradation of Dicamba and 2,4-D herbicides using simulated solar light. *Ceram Int* 40: 8701-8708.
15. JN Hasnidawani (2016) Synthesis of ZnO nanostructures using sol-gel method. *Proc Chem* l: 211-216.
16. EDESSGIIBI Barashkov N.D (2010) Electrochemical chlorine-free AC disinfection of water contaminated with *Salmonella typhimurium* bacteria. *Russ J Electrochem* 46: 306-311.
17. Q M C C F S D B A Martinez-Huitle CA (2004)Electrochemical incineration of chloroanilic acid using Ti/IRO_2, Pb/PbO_2 and Si/BDD electrodes. *Electrochim Acta* 949-956.
18. Q P Z J S T H H Zang L (1997) Photocatalytic bleaching of p-nitrosodimethylaniline in TiO*2* aqueous suspensions: A kinetic treatment involving some primary events photoinduced on the particle surface. *J Mol Catal A* 235-245.
19. Muff J, Bennedsen LR, Sogaard EG (2011) Study of electrochemical bleaching of p-nitrosodimethylaniline and its role of hydroxyl radical probe compound. *J Appl Electrochem* 41: 599-607.
20. T S H M B E Ramires-Sanchez I.M. (2017) Resource efficiency analysis for photocatalytic degradation and mineralization of estriol using TiO_2 nanoparticles. *Chemosphere* 1270-1285, M
21. M J B L K K S E Simonsen M.E. (2010) Photocatalytic bleaching of p-nitrosodimethylaniline and a comparison to the performance of other AOP technologies. *J Photochem Photobiol A* 244-249.
22. C T I Kraljic (1965) p-nitrosodimethylaniline as an OH radical scavenger in radiation chemistry. *J Am Chem Soc* 87: 2547-2550.
23. Fahataziz A (1977) Selected specific rates of reactions of transient form water in aqueous solutions III: Hydroxyl radical and pehydroxyl radical and their radical ions. Washington, 1977.
24. M C S M Bors W (1979) On the nature of biochemically generated hydroxyl radicals. *European J Biochem* 621-627.
25. MT Madigan, JM Martinko, DA Stahl and D. P. Clark Brock, Biology of Microorganisms, New York: Pearson Higher Education, 2011.
26. JL Sánchez-Salas, ML Santiago-Lara, B Setlow, et al. (1992) Properties of *Bacillus megaterium* and *Bacillus subtilis* mutants which lack the protease that degrades small, acid-soluble proteins during spre germination. *J Bacteriol* 174: 807-814.

27. Jones N, Ray B, Ranjit KT, et al. (2008) Antibacterial activity of ZnO nanoparticle suspensions on a broad spectrum of microorganism. *FEMS Microbiol Lett* 279: 71-76.
28. Sirelkhatim A, Mahmud S, Seeni A, et al. (2015) Review on zinc oxide nanoparticles: antibacterial activity and toxicity mechanism. *Nano Micro Lett* 7: 219-242.
29. J Achouri, S Corbel, A Aboulaich, et al. (2014) Aqueous synthesis and enhanced photocatalytic activity of ZnO/Fe_2O_3 heterostructures. *J Phys Chem Solids* 75: 1081-1087.
30. Setlow P (2011) Resistance of SPores of *Bacillus* Species to Ultraviolet Light. *Environ Mol Mutagen* 38: 97-104.
31. N Vermeulen, WJ Keeler, K Nandakumar, et al. (2007) The bactericidal effect of ultraviolet and visible light on *Escherichia coli*. *Biotechnol Bioeng* 99: 550-556.